SCIENCE CHINA
Information Sciences

• RESEARCH PAPER •

September 2023, Vol. 66 192304:1–192304:15
https://doi.org/10.1007/s11432-023-3799-6

Performance analysis of active RIS-aided multi-pair full-duplex communications with spatial correlation and imperfect CSI

Zhangjie PENG[1], Xueya LIU[1], Xue LIU[1], Cunhua PAN[2*], Xianzhe CHEN[1] & Hong REN[2]

[1]*College of Information, Mechanical and Electrical Engineering, Shanghai Normal University, Shanghai* 200234*, China;*
[2]*National Mobile Communications Research Laboratory, Southeast University, Nanjing* 210096*, China*

Received 4 March 2023/Revised 23 May 2023/Accepted 6 June 2023/Published online 28 August 2023

Abstract This paper investigates a multi-pair full-duplex (FD) communication system aided by an active reconfigurable intelligent surface (RIS) with spatial correlation and imperfect channel state information (CSI). We apply the linear minimum mean square error (LMMSE) method to estimate the cascaded user-RIS-user channel. The approximation for the sum achievable rate (ACR) is derived in closed form over correlated Rician fading channels. To provide insights in a poor-scattering environment, the sum ACR limits are also given when the Rician factors grow infinite. Subsequently, a method based on a genetic algorithm (GA) is designed for the sum ACR maximization considering the cases of continuous and discrete phase shifts. Simulation results validate the derived results, and present that the sum ACRs in the active RIS system are higher than the passive counterparts with the same power consumption, which indicates the superiority of the active RIS in overcoming the "multiplicative fading" effect.

Keywords RIS, active RIS, FD communication, spatial correlation, imperfect CSI

Citation Peng Z J, Liu X Y, Liu X, et al. Performance analysis of active RIS-aided multi-pair full-duplex communications with spatial correlation and imperfect CSI. Sci China Inf Sci, 2023, 66(9): 192304, https://doi.org/10.1007/s11432-023-3799-6

1 Introduction

Owing to the emergence of the booming applications, future communication networks are expected to realize high quality service requirements, such as extreme connectivity [1], ultra-reliable low latency communication [2], seamless global coverage [3], and massive data transmission [4]. In the beyond 5G wireless communication area, the technology of the reflective radio has attracted extensive attention as one of the state-of-the-art techniques to design spectral and energy efficient communication systems [5–7]. To meet the increasing demands for modern network traffic, the reconfigurable intelligent surface (RIS) has been introduced to assist wireless communications [8, 9]. The RIS integrates many programmable reflecting elements (REs) that is treated as a burgeoning meta-material to boost the signal quality at the receivers [10, 11] and extend the wireless coverage [12]. To be specific, the wireless communication environment can be reshaped by independently inducing the phase shift at each RE [13]. Accordingly, the desired signal can be steered to a desired direction while the interference signals can be weakened [14].

Recently, RIS has been integrated with the full-duplex (FD) communication technology [15–18]. FD communication supports bidirectional and simultaneous data transmission within the same frequency band, which is theoretically capable of doubling the data rate and improving the spectral efficiency [19]. The application of RIS in FD communication was investigated for the suppression of the interference between the transmit and the receive antennas in [15], and was proved efficient for mitigating different interferences in [16]. The RIS with plenty of REs can remarkably reduce the performance degradation

* Corresponding author (email: cpan@seu.edu.cn)

caused by residual interferences in FD transmission [17]. In [18], the RIS was deployed to cover the dead zone and ensure the user fairness of an FD communication network.

The considered RIS in [11–18], which is called passive RIS, does not require radio frequency (RF) chains or amplifiers, thus it greatly reduces the hardware cost and power consumption. Nevertheless, the "multiplicative fading" effect is non-negligible since the signal experiences double attenuation of the cascaded channel in the RIS-aided communication systems [20]. Thus, the passive RIS obtains constrained performance improvement. Recently, the active RIS has been proposed to break through the performance bottleneck [20]. Specifically, supported by low-power reflection-type amplifiers [21], the active RIS simultaneously reflects and amplifies the incident signal, acting as a remedy for the "multiplicative fading" effect at the price of additional power consumption. In [22], a cost-effective structure of REs was designed for the active RIS. The authors in [23] studied the single-input single-output system aided by active/passive RIS under the same power budget, and demonstrated that the active RIS performs better with a small number of REs. In [24], an active RIS was deployed for achievable rate (ACR) enhancement in a single-input multiple-output system. The maximum computational latency was minimized in a mobile edge computing system with the aid of the active RIS under the same power budget [25]. The authors in [26] optimized the transmit beamforming vector and the reflecting matrix of the active RIS to achieve a higher secrecy rate in a multi-antenna wiretap system.

However, we note that the RIS-related channels are usually correlated since the REs are closely packed due to physical constraints [27, 28]. In [27], a practical model was proposed for the RIS-related channels considering spatial correlation. The authors in [28] derived the approximate lower bound expression for the ACR in closed form in an RIS-aided massive multiple-input multiple-output system over correlated Rician channels with imperfect channel state information (CSI) and electromagnetic interference.

Against the above background, we investigate an active RIS-aided multi-pair FD communication system over spatially correlated channels relying on imperfect CSI. The main contributions are summarized below: (1) The linear minimum mean square error (LMMSE) method is applied to estimate the cascaded user-RIS-user channel. Then, the tractable expressions of the approximate sum ACRs are derived over correlated Rician fading channels with imperfect/perfect CSI; (2) The asymptotic expressions of the ACRs are obtained in pure line-of-sight (LoS) channels. Besides, we optimize the phase shifts by exploiting the genetic algorithm (GA); (3) Simulation results demonstrate the correctness of our derivations and the significance of the phase shifts design. We also draw comparisons of the sum ACRs between the active RIS system and the passive RIS system.

2 System model

We investigate an active RIS-assisted multi-pair FD communication system as shown in Figure 1. Denote the l-th user-pair as U_{2l-1} (on side A) and U_{2l} (on side B) for $\forall l = 1, \ldots, K$. Each user is equipped with one transmit antenna and one receive antenna. And we assume that the direct link between side A and side B is not available owing to the severe shadowing effects. Therefore, the active RIS acts as a remedy against the blockage, which is equipped with $N = N_{\mathrm{H}} \times N_{\mathrm{V}}$ REs. N_{H} and N_{V} are the number of REs per row and per column. Let ϕ_n and η_n respectively denote the phase shift and the amplification factor of the n-th RE. The phase shift matrix is $\boldsymbol{\Phi} = \mathrm{diag}(\mathrm{e}^{\mathrm{j}\phi_1}, \ldots, \mathrm{e}^{\mathrm{j}\phi_n}, \ldots, \mathrm{e}^{\mathrm{j}\phi_N})$, and $\boldsymbol{\Lambda} = \mathrm{diag}\left(\eta_1, \ldots, \eta_n, \ldots, \eta_N\right)$ represents the amplification factor matrix. The thermal noise $\boldsymbol{n}_{\mathrm{F}} \in \mathbb{C}^{N\times 1}$ introduced by the active elements is non-negligible, and it is modeled as $\boldsymbol{n}_{\mathrm{F}} \sim \mathcal{CN}\left(\boldsymbol{0}, \sigma_{\mathrm{F}}^2 \boldsymbol{I}_N\right)$.

2.1 Spatially correlated channel model

The channels from the transmit antenna of U_i $(i = 1, \ldots, 2K)$ to the active RIS and from the active RIS to the receive antenna of U_i are respectively denoted as $\boldsymbol{g}_{ti} \in \mathbb{C}^{N\times 1}$ and $\boldsymbol{g}_{ri} \in \mathbb{C}^{N\times 1}$, which are assumed to follow the spatially correlated Rician fading

$$\boldsymbol{g}_{xi} = \bar{\boldsymbol{g}}_{xi} + \boldsymbol{R}_{xi}^{\frac{1}{2}} \tilde{\boldsymbol{g}}_{xi}, \tag{1}$$

where $x \in \{r, t\}$. $\bar{\boldsymbol{g}}_{xi}$ is the LoS component under the uniform planar array model, which is given by

$$\bar{\boldsymbol{g}}_{xi} = \sqrt{\frac{\alpha_{xi}\mu_{xi}}{1+\mu_{xi}}} \boldsymbol{a}\left(\theta_{xi}^{\mathrm{a}}, \theta_{xi}^{\mathrm{e}}\right), \tag{2}$$

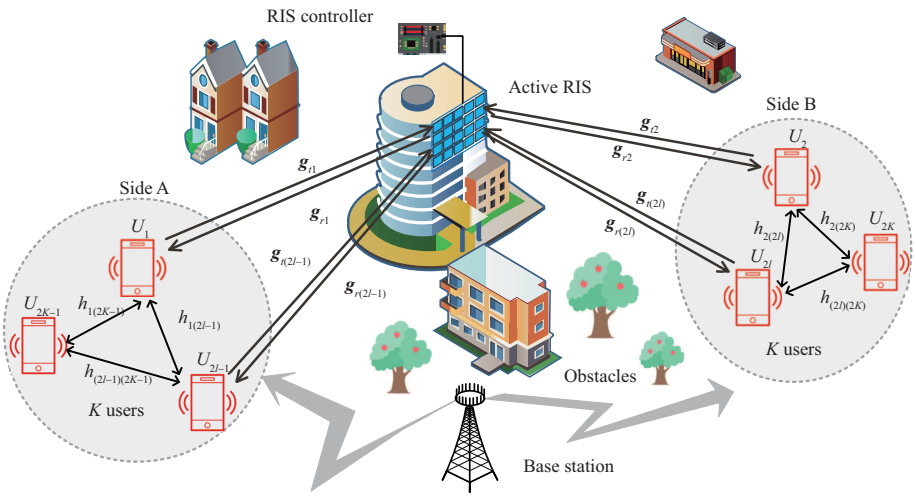

Figure 1 (Color online) Model of an active RIS-assisted multi-pair FD communication system.

where α_{xi} represents the large-scale fading coefficient, and μ_{xi} represents the Rician factor. θ^{a}_{xi} and θ^{e}_{xi} stand for the azimuth and elevation angles, respectively. The array response vector $\boldsymbol{a}(x,y) \in \mathbb{C}^{N\times 1}$ is

$$\boldsymbol{a}(x,y) = \left[1, \ldots, \mathrm{e}^{\mathrm{j}\frac{2\pi}{\lambda}(v_1(n)d_{\mathrm{H}}\sin x\cos y + v_2(n)d_{\mathrm{V}}\sin y)}, \ldots, \mathrm{e}^{\mathrm{j}\frac{2\pi}{\lambda}((N_{\mathrm{H}}-1)d_{\mathrm{H}}\sin x\cos y + (N_{\mathrm{V}}-1)d_{\mathrm{V}}\sin y)}\right]^{\mathrm{T}}, \tag{3}$$

where $v_1(n) = \mathrm{mod}(n-1, N_{\mathrm{H}})$, $v_2(n) = \lfloor (n-1)/N_{\mathrm{H}} \rfloor$ and λ is the carrier wavelength. Note that $\mathrm{mod}(x)$ denotes the modulus operation and $\lfloor x \rfloor$ truncates the argument. d_{H} and d_{V} stand for the width and length of each RE. Since the REs are tightly arranged, d_{H} and d_{V} also represent the horizontal and the vertical element-spacing, respectively. Additionally, $\tilde{\boldsymbol{g}}_{xi}$ stands for the small fading component and $\boldsymbol{R}_{xi}$ characterizes the spatial correlation whose (p,q)-th element is modelled as [24]

$$[\boldsymbol{R}_{xi}]_{p,q} \triangleq r_{pq} = \mathrm{sinc}\left(\frac{2||\boldsymbol{u}_p - \boldsymbol{u}_q||}{\lambda}\right), \tag{4}$$

where $\mathrm{sinc}(x) = \sin(\pi x)/(\pi x)$ and $\boldsymbol{u}_n = [0, v_1(n)d_{\mathrm{H}}, v_2(n)d_{\mathrm{V}}]^{\mathrm{T}}$.

Besides, we assume that the direct links only exist between the users on the same side due to the short communication distance. When U_i and U_k are on the same side, and the channel between them is denoted as $h_{ik}(\{i,\ k\} \in \mathcal{S}_k,\ i \neq k)$, where $\mathcal{S}_k = \{1, 3, \ldots, 2K-1\}$ when k is odd and $S_k = \{2, 4, \ldots, 2K\}$ when k is even. Particularly, h_{ii} represents the loop channel between the transmit and receive antenna of U_i. The channels h_{ik} and h_{ii} follow typical Rayleigh fading [29], i.e., $h_{ik} \sim \mathcal{CN}(0, \beta_{ik})$ and $h_{ii} \sim \mathcal{CN}(0, \beta_{ii})$.

2.2 Channel estimation and data transmission

The accurate CSI is crucial but difficult to obtain, especially in RIS-related channels for lack of the RF chains [30], which means we cannot estimate the user-RIS channel and RIS-user channel separately. Instead, the CSI of the cascaded user-RIS-user channel can be acquired. We denote the cascaded channel from the transmitter $U_{i'}$ to the receiver U_i through the active RIS as $q_{ii'}$, and it is written as

$$q_{ii'} = \boldsymbol{g}_{ri}^{\mathrm{T}} \boldsymbol{\Phi} \boldsymbol{\Lambda} \boldsymbol{g}_{ti'}. \tag{5}$$

The users simultaneously transmit orthogonal pilot sequences of τ symbols with power τp where $\tau \geqslant 2K$. We denote $\boldsymbol{S} = [\boldsymbol{s}_1, \ldots, \boldsymbol{s}_{2K}] \in \mathbb{C}^{\tau\times 2K}$ as the pilot matrix of all users, where $\boldsymbol{s}_i \in \mathbb{C}^{\tau\times 1}$ is the pilot sequence transmitted from user U_i. Note that $\boldsymbol{S}^{\mathrm{H}}\boldsymbol{S} = \boldsymbol{I}_{2K}$.

The pilot signal received at U_i is given by

$$\boldsymbol{x}_i^{\mathrm{H}} = \sqrt{\tau p}\boldsymbol{g}_{ri}^{\mathrm{T}}\boldsymbol{\Phi}\boldsymbol{\Lambda}\boldsymbol{G}_t\boldsymbol{\Upsilon}_i\boldsymbol{S}^{\mathrm{H}} + \sqrt{\tau p \rho_{\mathrm{L}}}h_{ii}\boldsymbol{s}_i^{\mathrm{H}} + \sum_{\{k,i\}\in S_k, k\neq i}\sqrt{\tau p}h_{ik}\boldsymbol{s}_k^{\mathrm{H}} + \boldsymbol{g}_{ri}^{\mathrm{T}}\boldsymbol{\Phi}\boldsymbol{\Lambda}\boldsymbol{N}_{\mathrm{F}} + \boldsymbol{n}_i^{\mathrm{H}}, \tag{6}$$

where $\boldsymbol{x}_i^{\mathrm{H}} \in \mathbb{C}^{1\times\tau}$, $\boldsymbol{G}_t = [\boldsymbol{g}_{t1}, \ldots, \boldsymbol{g}_{t2K}] \in \mathbb{C}^{N\times 2K}$ is the transmit channel matrix of all users. $\boldsymbol{\Upsilon}_i = \mathrm{diag}(1, \ldots, \sqrt{\rho_{\mathrm{S}}}, \ldots, 1) \in \mathbb{C}^{2K\times 2K}$ where the i-th element of the matrix $\boldsymbol{\Upsilon}_i$ is $\sqrt{\rho_{\mathrm{S}}}$ and the other elements

are 1. ρ_{L} and ρ_{S} indicate the loop-interference (LI) and self-interference (SI) coefficients satisfying $0 < \rho_{\mathrm{L}}, \rho_{\mathrm{S}} \leqslant 1$. $\boldsymbol{N}_{\mathrm{F}} = [\boldsymbol{n}_{\mathrm{F},1}, \ldots, \boldsymbol{n}_{\mathrm{F},\tau}] \in \mathbb{C}^{N\times\tau}$ is the thermal noise matrix introduced by the active RIS, and $\boldsymbol{n}_i^{\mathrm{H}} \in \mathbb{C}^{1\times\tau}$ is the static noise vector at U_i. Then, by multiplying (6) with $\frac{\boldsymbol{s}_{i'}}{\sqrt{\tau p}}$, the observation scalar for $U_{i'}$ is obtained as

$$\begin{aligned} y_i^{\mathrm{p}} &= \frac{1}{\sqrt{\tau p}}\boldsymbol{x}_i^{\mathrm{H}}\boldsymbol{s}_{i'} \\ &= \boldsymbol{g}_{ri}^{\mathrm{T}}\boldsymbol{\Phi}\boldsymbol{\Lambda}\boldsymbol{G}_t\boldsymbol{\Upsilon}_i\boldsymbol{S}^{\mathrm{H}}\boldsymbol{s}_{i'} + \sqrt{\rho_{\mathrm{L}}}h_{ii}\boldsymbol{s}_i^{\mathrm{H}}\boldsymbol{s}_{i'} + \sum_{\{k,i\}\in S_k, k\neq i} h_{ik}\boldsymbol{s}_k^{\mathrm{H}}\boldsymbol{s}_{i'} + \frac{1}{\sqrt{\tau p}}\boldsymbol{g}_{ri}^{\mathrm{T}}\boldsymbol{\Phi}\boldsymbol{\Lambda}\boldsymbol{N}_{\mathrm{F}}\boldsymbol{s}_{i'} + \frac{1}{\sqrt{\tau p}}\boldsymbol{n}_i^{\mathrm{H}}\boldsymbol{s}_{i'} \\ &= q_{ii'} + \frac{1}{\sqrt{\tau p}}\boldsymbol{g}_{ri}^{\mathrm{T}}\boldsymbol{\Phi}\boldsymbol{\Lambda}\boldsymbol{N}_{\mathrm{F}}\boldsymbol{s}_{i'} + \frac{1}{\sqrt{\tau p}}\boldsymbol{n}_i^{\mathrm{H}}\boldsymbol{s}_{i'}. \end{aligned} \tag{7}$$

Then, we use the LMMSE method to estimate the cascaded channel $q_{ii'}$ as follows.

Theorem 1. The LMMSE estimation of the cascaded channel $q_{ii'}$ is derived as

$$\hat{q}_{ii'} = \epsilon_{ii'} + \iota_{ii'}\left(q_{ii'} + \frac{\boldsymbol{g}_{ri}^{\mathrm{T}}\boldsymbol{\Theta}\boldsymbol{\Lambda}\boldsymbol{N}_{\mathrm{F}}\boldsymbol{s}_{i'}}{\sqrt{\tau p}} + \frac{\boldsymbol{n}_i^{\mathrm{H}}\boldsymbol{s}_{i'}}{\sqrt{\tau p}} - \epsilon_{ii'}\right), \tag{8}$$

where

$$\epsilon_{ii'} \triangleq \bar{\boldsymbol{g}}_{ri}^{\mathrm{T}}\boldsymbol{\Phi}\boldsymbol{\Lambda}\bar{\boldsymbol{g}}_{ti'}, \quad \psi_{ii'} \triangleq \frac{\alpha_{ri}\alpha_{ti'}\mu_{ri}\mu_{ti'}}{(1+\mu_{ri})(1+\mu_{ti'})}, \tag{9}$$

$$\iota_{ii'} \triangleq \frac{\eta^2\psi_{ii'}(\frac{1}{\mu_{ti'}}\hat{\Omega}_{ri} + \frac{1}{\mu_{ri}}\hat{\Omega}_{ti'} + \frac{1}{\mu_{ri}\mu_{ti'}}\hat{\Omega}_0)}{\eta^2\psi_{ii'}(\frac{1}{\mu_{ti'}}\hat{\Omega}_{ri} + \frac{1}{\mu_{ri}}\hat{\Omega}_{ti'} + \frac{1}{\mu_{ri}\mu_{ti'}}\hat{\Omega}_0) + \frac{N\sigma_{\mathrm{F}}^2\eta^2\alpha_{ri}}{\tau p} + \frac{\sigma_i^2}{\tau p}}, \tag{10}$$

$\hat{\Omega}_{xi}$ and $\hat{\Omega}_0$ are respectively defined in (A12) and (A16) in Appendix A, $x \in \{r, t\}$.

Proof. See Appendix A.

And the received signal of user U_i is expressed as

$$\begin{aligned} y_i = &\underbrace{\sqrt{P_{i'}}\hat{q}_{ii'}s_{i'}}_{\text{desired signal}} + \underbrace{\sqrt{P_{i'}}(q_{ii'} - \hat{q}_{ii'})\,s_{i'}}_{\text{estimation error}} + \underbrace{\sum_{k\neq i,i'}^{2K}\sqrt{P_k}q_{ik}s_k}_{\text{inter-pair interference}} + \underbrace{\sqrt{\rho_{\mathrm{S}}}\sqrt{P_i}q_{ii}s_i}_{\text{self interference}} \\ &+ \underbrace{\sqrt{\rho_{\mathrm{L}}}\sqrt{P_i}h_{ii}s_i}_{\text{loop interference}} + \underbrace{\sum_{\{k,i\}\in\mathcal{S}_k, k\neq i}\sqrt{P_k}h_{ik}s_k}_{\text{inter-user interference}} + \underbrace{\boldsymbol{g}_{ri}^{\mathrm{T}}\boldsymbol{\Lambda}\boldsymbol{\Phi}\boldsymbol{n}_{\mathrm{F}}}_{\text{dynamic noise}} + n_i, \end{aligned} \tag{11}$$

where s_i is the information symbol sent from U_i with power P_i. $n_i \sim \mathcal{CN}(0, \sigma_i^2)$ is the additive white Gaussian noise (AWGN).

Based on (11), the signal-to-interference-plus-noise ratio (SINR) at U_i is given by

$$\gamma_i = \frac{P_{i'}\left|\hat{q}_{ii'}\right|^2}{P_{i'}\left|q_{ii'} - \hat{q}_{ii'}\right|^2 + \sum_{k\neq i'}^{2K}\rho_1 P_k\left|q_{ik}\right|^2 + \sum_{\{k,i\}\in\mathcal{S}_k}\rho_2 P_k\left|h_{ik}\right|^2 + \left\|\boldsymbol{g}_{ri}^{\mathrm{T}}\boldsymbol{\Lambda}\boldsymbol{\Phi}\right\|^2\sigma_{\mathrm{F}}^2 + \sigma_i^2}, \tag{12}$$

where $\rho_1 = \begin{cases}\rho_{\mathrm{S}}, & k = i,\\ 1, & k \neq i,\end{cases}$ and $\rho_2 = \begin{cases}\rho_{\mathrm{L}}, & k = i,\\ 1, & k \neq i.\end{cases}$

The sum ACR can be derived as

$$R = \frac{T-\tau}{T}\sum_{i=1}^{2K}R_i = \frac{T-\tau}{T}\sum_{i=1}^{2K}\mathbb{E}\{\log_2(1+\gamma_i)\}, \tag{13}$$

where T stands for the coherence interval length.

2.3 Total power consumption

The amplification power of the active RIS is given by

$$P_{\mathrm{R}} = \sum_{i=1}^{2K} P_i \mathbb{E}\{\|\boldsymbol{\Lambda}\boldsymbol{\Phi}\boldsymbol{g}_{ti}\|^2\} + \mathbb{E}\{\|\boldsymbol{\Lambda}\boldsymbol{\Phi}\boldsymbol{n}_{\mathrm{F}}\|^2\}. \tag{14}$$

The total power consumed in the active RIS system is

$$P_{\mathrm{A}} = \sum_{i=1}^{2K} P_i + \varepsilon^{-1} P_{\mathrm{R}} + N(P_{\mathrm{DC}} + P_{\mathrm{SW}}), \tag{15}$$

where ε is the amplifier efficiency, P_{DC} and P_{SW} respectively stand for the direct current biasing power and the power consumed by the switch and control circuit at each RE [18]. The total power consumption of the passive RIS system is $P_{\mathrm{P}} = \sum_{i=1}^{2K} P_i' + NP_{\mathrm{SW}}$ where P_i' is the transmit power of U_i in the passive RIS system. If $P_{\mathrm{A}} \leqslant N(P_{\mathrm{DC}} + P_{\mathrm{SW}})$ (or $P_{\mathrm{P}} \leqslant NP_{\mathrm{SW}}$), the active RIS (or passive RIS) does not work, and the sum ACR is zero. In this paper, we assume that $P_{\mathrm{A}} = P_{\mathrm{P}} = P$ for fairness.

3 ACR analysis

In this section, the approximate expressions of the sum ACRs are derived in closed form for the considered active RIS-aided multi-pair FD communication system over correlated Rician channels relying on imperfect/perfect CSI. Then, we provide more insights in some special cases when the Rician factors grow infinite. First of all, the amplification factor is obtained as follows.

Lemma 1. Assuming that the amplification factors are the same, i.e., $\eta_n = \eta$, $\forall n$, we have

$$\eta^2 = \frac{P_{\mathrm{R}}}{\sum_{i=1}^{2K} NP_i\alpha_{ti} + N\sigma_{\mathrm{F}}^2}. \tag{16}$$

Proof. See Appendix B.

According to Theorem 1, Eq. (13), and Lemma 1, the approximate sum ACR is derived below.

Theorem 2. For an active RIS-aided multi-pair FD communication system, the approximate expression of the sum ACR over spatially correlated Rician fading channels and imperfect CSI is given by

$$R \approx \tilde{R} = \frac{T-\tau}{T} \sum_{i=1}^{2K} \log_2(1+\tilde{\gamma}_i), \tag{17}$$

where

$$\tilde{\gamma}_i = \frac{P_{i'}(\eta^2\varsigma_{ii'} + |\iota_{ii'}|^2(\frac{N\sigma_{\mathrm{F}}^2\eta^2\alpha_{ri}}{\tau p} + \frac{\sigma_i^2}{\tau p}))}{P_{i'}(\eta^2\varrho_{ii'} + |\iota_{ii'}|^2(\frac{N\sigma_{\mathrm{F}}^2\eta^2\alpha_{ri}}{\tau p} + \frac{\sigma_i^2}{\tau p})) + \sum_{k\neq i'}^{2K} P_k\eta^2\rho_1\xi_{ik} + \sum_{\{k,i\}\in\mathcal{S}_k} P_k\rho_2\beta_{ik} + N\eta^2\alpha_{ri}\sigma_{\mathrm{F}}^2 + \sigma_i^2}, \tag{18}$$

$$\xi_{ik} \triangleq \psi_{ik}\left(\bar{\Omega}_{ik} + \left(\frac{1}{\mu_{tk}}\hat{\Omega}_{ri} + \frac{1}{\mu_{ri}}\hat{\Omega}_{tk} + \frac{1}{\mu_{ri}\mu_{tk}}\hat{\Omega}_0\right)\right), \tag{19}$$

$$\varsigma_{ii'} \triangleq \psi_{ii'}\left(\bar{\Omega}_{ii'} + |\iota_{ii'}|^2\left(\frac{1}{\mu_{ti'}}\hat{\Omega}_{ri} + \frac{1}{\mu_{ri}}\hat{\Omega}_{ti'} + \frac{1}{\mu_{ri}\mu_{ti'}}\hat{\Omega}_0\right)\right), \tag{20}$$

$$\varrho_{ii'} \triangleq \xi_{ii'} + \varsigma_{ii'} - 2\left((1-\iota_{ii'})\,\psi_{ii'}\bar{\Omega}_{ii'} + \iota_{ii'}\xi_{ii'}\right) \tag{21}$$

with $\bar{\Omega}_{ii'}$ defined in (A9).

Proof. See Appendix C.

According to Theorem 2, the ACR of l-th user-pair increases when the channel fading reduces for the l-th user-pair (through enlarging $\alpha_{x(2l-1)}$ and $\alpha_{x(2l)}$), and decreases when the channel fading reduces for other user-pairs except the l-th user-pair (through enlarging $\alpha_{x(2l'-1)}$ and $\alpha_{x(2l')}$ for $l' \neq l$).

Corollary 1. When $\tau \to \infty$, we have $\hat{q}_{ii'} \to q_{ii'}$. Similar to the imperfect CSI case, the approximation of the sum ACR in the active RIS system with perfect CSI is derived as

$$\begin{aligned}\tilde{R}^{\mathrm{P}} &= \sum_{i=1}^{2K} \log_2(1+\tilde{\gamma}_i^{\mathrm{P}}) \\ &= \sum_{i=1}^{2K} \log_2\left(1+\frac{P_{i'}\eta^2\xi_{ii'}}{\sum_{k\neq i'}^{2K}\rho_1 P_k\eta^2\xi_{ik}+\sum_{\{k,i\}\in\mathcal{S}_k}P_k\rho_2\beta_{ik}+N\eta^2\alpha_{ri}\sigma_{\mathrm{F}}^2+\sigma_i^2}\right).\end{aligned} \tag{22}$$

Proof. According to Theorem 2, if $\tau \to \infty$, we have $\frac{1}{\tau p} \to 0$. We can further derive that $\iota_{ii'} \to 1$, $\varsigma_{ii'} \to \xi_{ii'}$ and $\varrho_{ii'} \to 0$. Substituting these results into (18)–(21), the sum ACR in the active RIS system relying on perfect CSI is obtained.

Note that $\tilde{R}^{\mathrm{P}}$ in Corollary 1 is higher in comparison to $\tilde{R}$ (i.e., the counterpart with imperfect CSI in Theorem 2) since the channels are well-conditioned.

When the environment has few scatters, i.e., the Rician factors grow without bound, only LoS components exist. Then, the asymptotic expression of the sum ACR in the active RIS system with pure LoS channels and imperfect CSI is given below.

Corollary 2. If the Rician factors $\mu_{ti} = \mu_{ti'} = \mu_{ri} = \mu_{ri'} \to \infty$, $\forall i, i'$, the sum ACRs in the active RIS system with imperfect and perfect CSI respectively converge to $\bar{R}$ in (23) and $\bar{R}^{\mathrm{P}}$ in (24).

$$\tilde{R} \to \bar{R} = \frac{T-\tau}{T}\sum_{i=1}^{2K}\log_2\left(1+\bar{\gamma}_i\right), \tag{23}$$

$$\tilde{R}^{\mathrm{P}} \to \bar{R}^{\mathrm{P}} = \sum_{i=1}^{2K}\log_2\left(1+\bar{\gamma}_i^{\mathrm{P}}\right), \tag{24}$$

where

$$\bar{\gamma}_i = \bar{\gamma}_i^{\mathrm{P}} = \frac{P_{i'}\alpha_{ti'}\alpha_{ri}\bar{\Omega}_{ii'}}{\sum_{k\neq i'}^{2K}P_k\rho_1\alpha_{tk}\alpha_{ri}\bar{\Omega}_{ik}+\sum_{\{k,i\}\in\mathcal{S}_k}\frac{P_k\rho_2\beta_{ik}}{\eta^2}+N\alpha_{ri}\sigma_{\mathrm{F}}^2+\frac{\sigma_i^2}{\eta^2}}. \tag{25}$$

Corollary 2 indicates that when the active RIS is deployed properly in a poor-scattering environment, the approximation of the sum ACR will approach a nonzero constant value. Comparing (23) and (24), we reveal that with pure LoS channels, $\tilde{\gamma}_i$ in (17)and $\tilde{\gamma}_i^{\mathrm{P}}$ in (22) will converge to the same value regardless of the CSI quality, i.e., $\bar{\gamma}_i = \bar{\gamma}_i^{\mathrm{P}}$.

Corollary 3. For the passive RIS-aided multi-pair FD communication system, the approximate ACRs relying on imperfect CSI and perfect CSI are respectively given by $\tilde{R}^{\mathrm{Pas}}$ in (26) and $\tilde{R}^{\mathrm{Pas,P}}$ in (27).

$$\tilde{R}^{\mathrm{Pas}} = \frac{T-\tau}{T}\sum_{i=1}^{2K}\log_2\left(1+\frac{P_{i'}(\varsigma_{ii'}+\frac{|\iota_{ii'}^{\mathrm{Pas}}|^2\sigma_i^2}{\tau p})}{P_{i'}(\varrho_{ii'}^{\mathrm{Pas}}+\frac{|\iota_{ii'}^{\mathrm{Pas}}|^2\sigma_i^2}{\tau p})+\sum_{k\neq i'}^{2K}P_k\rho_1\xi_{ik}+\sum_{\{k,i\}\in\mathcal{S}_k}P_k\rho_2\beta_{ik}+\sigma_i^2}\right), \tag{26}$$

$$\tilde{R}^{\mathrm{Pas,P}} = \sum_{i=1}^{2K}\log_2\left(1+\frac{P_{i'}\xi_{ii'}}{\sum_{k\neq i'}^{2K}\rho_1 P_k\xi_{ik}+\sum_{\{k,i\}\in\mathcal{S}_k}P_k\rho_2\beta_{ik}+\sigma_i^2}\right), \tag{27}$$

where

$$\iota_{ii'}^{\mathrm{Pas}} \triangleq \frac{\psi_{ii'}(\frac{1}{\mu_{ti'}}\hat{\Omega}_{ri}+\frac{1}{\mu_{ri}}\hat{\Omega}_{ti'}+\frac{1}{\mu_{ri}\mu_{ti'}}\hat{\Omega}_0)}{\psi_{ii'}(\frac{1}{\mu_{ti'}}\hat{\Omega}_{ri}+\frac{1}{\mu_{ri}}\hat{\Omega}_{ti'}+\frac{1}{\mu_{ri}\mu_{ti'}}\hat{\Omega}_0)+\frac{\sigma_i^2}{\tau p}}, \tag{28}$$

$$\varrho_{ii'}^{\mathrm{Pas}} \triangleq \xi_{ii'}+\varsigma_{ii'}-2\left(\left(1-\iota_{ii'}^{\mathrm{Pas}}\right)\psi_{ii'}\bar{\Omega}_{ii'}+\iota_{ii'}^{\mathrm{Pas}}\xi_{ii'}\right). \tag{29}$$

Similar to Corollary 2, for the passive RIS system, the asymptotic expressions of the sum ACRs with pure LoS channels relying on imperfect CSI and perfect CSI are respectively given by $\bar{R}^{\mathrm{Pas}}$ in (30) and $\bar{R}^{\mathrm{Pas,P}}$ in (31).

$$\tilde{R}^{\mathrm{Pas}} \to \bar{R}^{\mathrm{Pas}} = \frac{T-\tau}{T}\sum_{i=1}^{2K}\log_2\left(1+\bar{\gamma}_i^{\mathrm{Pas}}\right), \tag{30}$$

$$\tilde{R}^{\mathrm{Pas,P}} \to \bar{R}^{\mathrm{Pas,P}} = \sum_{i=1}^{2K} \log_2\left(1+\bar{\gamma}_i^{\mathrm{Pas}}\right), \tag{31}$$

where

$$\bar{\gamma}_i^{\mathrm{Pas}} = \frac{P_{i'}\alpha_{ti'}\alpha_{ri}\bar{\Omega}_{ii'}}{\sum_{k\neq i'}^{2K} P_k\rho_1\alpha_{tk}\alpha_{ri}\bar{\Omega}_{ik} + \sum_{\{k,i\}\in\mathcal{S}_k} P_k\rho_2\beta_{ik} + \sigma_i^2}. \tag{32}$$

Corollary 4. When the users have the same transmit power (i.e., $P_i = P_{\mathrm{u}}, \forall i$) and the signal-to-noise ratio (SNR) $\frac{P_{\mathrm{u}}}{\sigma_i^2}$ is very high, the sum ACRs for the active RIS system relying on imperfect and perfect CSI respectively converge to $\dot{R}$ in (33) and $\dot{R}^{\mathrm{P}}$ in (34).

$$\tilde{R} \to \dot{R} = \frac{T-\tau}{T}\sum_{i=1}^{2K} \log_2\left(1+\bar{\gamma}_i^{\mathrm{u}}\right), \tag{33}$$

$$\tilde{R}^{\mathrm{P}} \to \dot{R}^{\mathrm{P}} = \sum_{i=1}^{2K} \log_2\left(1+\bar{\gamma}_i^{\mathrm{u}}\right), \tag{34}$$

where

$$\bar{\gamma}_i^{\mathrm{u}} = \frac{\eta^2\xi_{ii'}}{\sum_{k\neq i'}^{2K} \rho_1\eta^2\xi_{ik} + \sum_{\{k,i\}\in\mathcal{S}_k}\rho_2\beta_{ik}}. \tag{35}$$

Corollary 4 indicates that with high SNR, the sum ACRs for the active RIS system approach to different constants. We can also derive the asymptotic expressions of the sum ACRs for the passive RIS system by setting $\eta = 1$ in Corollary 4.

4 Optimization of RIS phase shifts

We propose a GA-based method to obtain the phase shifts design for maximizing the sum ACR in this section. The optimization problem is formulated below.

$$\max_{\mathbf{\Phi}} \ \tilde{R} \tag{36a}$$

$$\text{s.t.} \ \ \phi_n \in [0, 2\pi), \forall n, \ \text{or} \tag{36b}$$

$$\phi_n \in \left\{0, \frac{2\pi}{2^B}, \ldots, \left(2^B-1\right)\frac{2\pi}{2^B}\right\}, \forall n, \tag{36c}$$

where $\tilde{R}$ is given by Theorem 2, and B is the resolution bit. Note that Problem (36) is non-convex.

Due to the fact that the GA only needs the expression of the objective function and does not require complex mathematical derivations, it is suitable for solving the non-convex optimization problem. To be specific, GA is a heuristic search method simulating natural selection. During the searching process, GA searches for a cluster of solutions rather than just a single one, which can avoid falling into the local optimum. The proposed method is detailed as follows.

(1) Chromosome representation. We denote the n-th gene information as ϕ_n to represent the chromosomal characteristics.

(2) Fitness evaluation. Next, we evaluate the individuals with a fitness function, which is the only judging standard to evaluate the entire population. The fitness function is defined as

$$f(\mathbf{\Phi}) = \tilde{R}. \tag{37}$$

(3) Evolution strategy. We apply a roulette-wheel selection function for twice to obtain two candidates as parents. According to (37), the individuals with a higher fitness value are more likely to be chosen for the reason of "survival of the fittest" in natural selection. The algorithm of the selection function is in Algorithm 1 described on the top of the next page.

The next step is the crossover, which is designed to introduce variations into the new population by exchanging portions of their internal representation. We select the single-point crossover operation, and

Algorithm 1 Selection function

Input: The number of parents N_c;
Output: r'-th individual of the fitness value list;
Set a number s randomly within (0,1);
for $r = 1, \ldots, N_c$ **do**
  Calculate $C(r) = \sum_{i=0}^{r-1}(N_c - i)$;
end for
Calculate $C_p = \sum_{r=1}^{N_c} r$;
Define a vector $\boldsymbol{r} = [C(1)/C_p, \ldots, C(r)/C_p, \ldots, 1]$ to store the cumulative probabilities;
Find the maximum elements $C(r')/C_p$ closest to s and note down its index as r';
Select the r'-th individual as final result.

the crossing position is randomly adjusted. Take a binary chromosome representation as an example, two individuals $i_1 = 110 \cdot 10110$ and $i_2 = 010 \cdot 01110$ are about to crossover at the random point as indicated. The final results are $i_1' = 110 \cdot 01110$ and $i_2' = 010 \cdot 10110$.

After the crossover, there is a low probability of the genetic mutation occurring in individual, which is detailed in Algorithm 2. The mutation function is designed to produce the chromosomes that display new properties and avoid falling into the local optimum. Moreover, we note that the mutation function is applied on individuals except the elite to maintain the superiority of the population.

Algorithm 2 Mutation function

Initialization: The number of RIS units N, population size N_p and mutation rate m;
Calculate the number of genes to be mutated as $N_m = m \times (N_p - 1) \times N$;
Set a number s randomly within $(0, 1)$;
for $i = 1, \ldots, N_m$ **do**
  Identify the location point n' of mutated genes;
  Replace $\phi_{n'}$ randomly with (36b) or (36c);
end for
Update the information about the newly-mutated population.

The details of the proposed method are given in Algorithm 3, where both the continuous and discrete phase shifts are considered. The computational complexity of GA is $N_p \times t$, where N_p is the population size and t is the iteration number [31].

Algorithm 3 GA-based method for phase shifts optimization

Initialization: The iteration number t, the population size N_p, the number of RIS elements N, convergence precision ε, the maximum iteration number N_i;
Generate initial gene information ϕ_m according to (36b) or (36c);
for $t = 1, \ldots, N_i$ **do**
  while $\frac{\bar{f}_{\text{fit}}(t) - \bar{f}_{\text{fit}}(t-1)}{\bar{f}_{\text{fit}}(t-1)} > \varepsilon$ **do**
    for $p = 1, \ldots, N_p$ **do**
      Calculate the fitness value $f_{\text{fit}}(p) = f(\boldsymbol{\Phi}_{p,t})$ of the p-th individual $\boldsymbol{\Phi}_{p,t}$ according to (37);
    end for
    Rank all individuals on the basis of the fitness value to find an elite $\boldsymbol{\Phi}_{e,t}$;
    Use Algorithm 1 to generate a pair of parent chromosomes of the mating pool;
    Crossover the parent chromosomes to get children chromosomes;
    Use Algorithm 2 on the current generation except $\boldsymbol{\Phi}_{e,t}$;
    Calculate the average fitness value of the current generation as $\bar{f}_{\text{fit}}(t) = \sum_{p=1}^{N_p} \frac{1}{N_p} f_{\text{fit}}(p)$;
    Set $\bar{f}_{\text{fit}}(t) = \bar{f}_{\text{fit}}(t+1)$;
  end while
end for
Output: The iteration number t, the elite $\boldsymbol{\Phi}_{e,t}$ of the current generation.

5 Numerical results

Simulation results are presented to validate the derived results of the sum ACRs. We set $\rho_{\text{S}} = \rho_{\text{L}} = 0.1$, $\mu_{xi} = \mu_{xi'} = 10$, $K = 3$, $N = 16$, $P = 10$ W, $\kappa = 0.1$, $2KP_i = \kappa P$, $\sigma_{\text{F}}^2 = -70$ dBm [21], $\varepsilon = 0.8$, $P_{\text{SW}} = -10$ dBm, $P_{\text{DC}} = -5$ dBm [24], $\tau = 2K$, $\tau p = P_i$, $T = 196$, $\sigma_i^2 = -104$ dBm [28], α_{xi}, θ_{xi}^{a} and θ_{xi}^{e} are set according to [32]. The curves marked with "Simu" represent the simulations obtained by averaging 2000 Monte-Carlo realizations, whereas the curves marked with "Appro" represent the approximations.

Figure 2 depicts the sum ACRs versus P in active RIS system and passive RIS system with random and optimized phase shifts. First, it is clear that the approximate expressions match well with the simulation

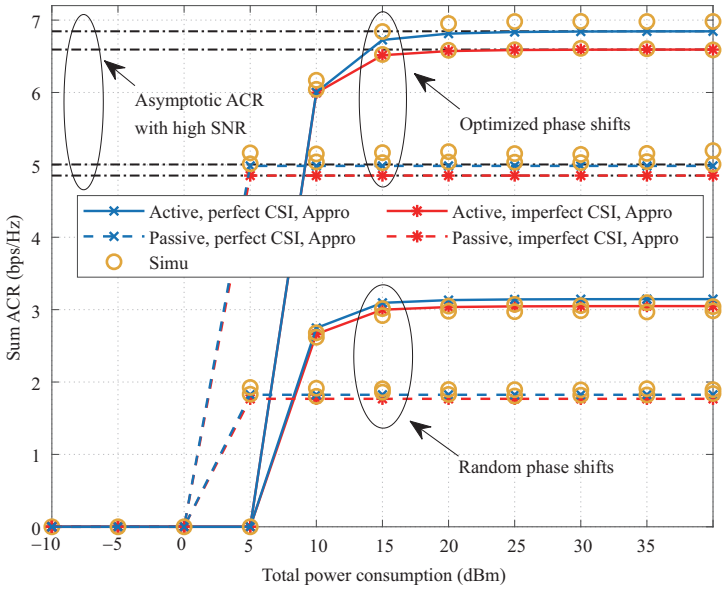

Figure 2 (Color online) Sum ACRs versus P in both active RIS system and passive RIS system.

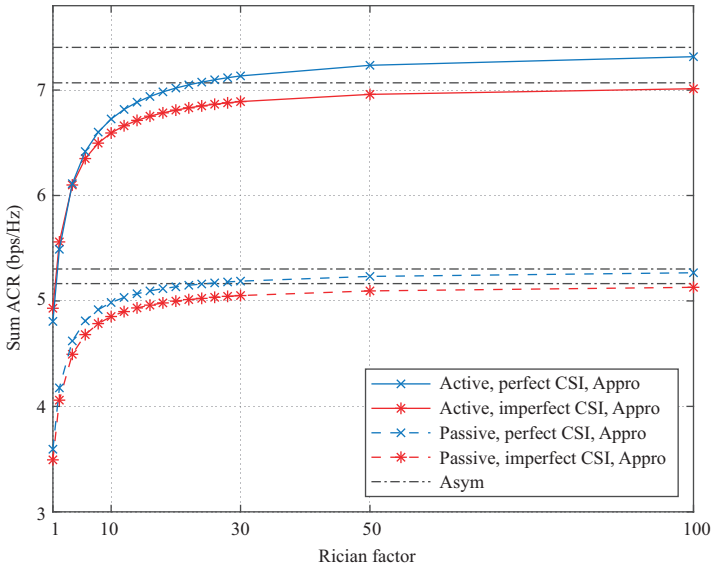

Figure 3 (Color online) Sum ACRs versus the Rician factor with the optimized phase shifts.

results, which verifies the correctness of our derivations. And we note that the sum ACRs are zero when P is too small to support the hardware power consumption. Besides, the sum ACRs with perfect CSI are higher in contrast to the imperfect counterpart since the CSI estimation errors deteriorate the system performance. And the GA-based method is effective on performance improvement in contrast to random phase shifts. Moreover, the sum ACRs converge to fixed values with high SNR, which verifies the derivations in Corollary 4.

Figure 3 investigates the sum ACRs versus the Rician factors with the optimized phase shifts. The curves marked with "Asym" stand for the asymptotic expressions derived in (23), (24), (30) and (31). The sum ACRs grow with the increase of the Rician factors at the outset and gradually converge, which indicates that the RIS achieves limited performance improvement in a rich-scattering environment. Thus, we should deploy the RIS in a high position with poor scattering.

Figure 4 illustrates the sum ACRs versus the resolution bit B with the optimized phase shifts. The curves marked with "Continuous" and "Discrete" are obtained by applying Algorithm 3 to Problem (36a) with the constraint (36b) and the constraint (36c), respectively. When the resolution bit of the RIS decreases, i.e., $B = 1$, the system performance obviously degrades. And we can observe that the optimized

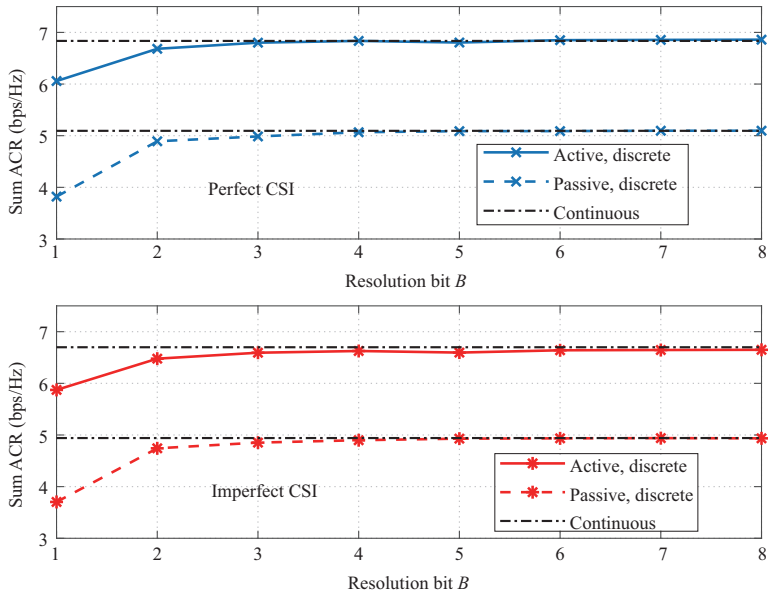

Figure 4 (Color online) Sum ACRs versus the resolution bit with the optimized phase shifts.

ACRs tend to the ACRs with the continuous phase shifts when B is greater than three. Thus, $B = 3$ is suitable for engineering design in practice since the continuous phase shifts are ideal.

6 Conclusion

In this paper, we derived the approximate expressions of the sum ACRs in closed form for the active RIS-aided multi-pair FD communication system with spatial correlation and imperfect CSI. The LMMSE estimation method was applied to obtain the CSI of the cascaded user-RIS-user channel. We analyzed the ACR with various contributing factors and derived the asymptotic expressions of the ACRs in pure LoS channels. The correctness of our derivations was confirmed through Monte-Carlo simulations. Moreover, we optimized the phase shifts with an effective GA-based method for both continuous and discrete cases to maximize the sum ACRs. And the active RIS showed its superiority over the passive RIS in overcoming the multiplicative-fading effect.

Acknowledgements This work of Zhangjie PENG was supported in part by Natural Science Foundation of Shanghai (Grant No. 22ZR1445600), National Natural Science Foundation of China (Grant No. 61701307), and Open Research Fund of National Mobile Communications Research Laboratory, Southeast University (Grant No. 2018D14). This work of Cunhua PAN was supported in part by National Natural Science Foundation of China (Grant No. 62201137) and Fundamental Research Funds for the Central Universities (Grant No. 2242022k60001). This work of Hong REN was supported in part by National Natural Science Foundation of China (Grant No. 62101128) and Basic Research Project of Jiangsu Provincial Department of Science and Technology (Grant No. BK20210205).

References

1 You X H. 6G extreme connectivity via exploring spatiotemporal exchangeability. Sci China Inf Sci, 2023, 66: 130306
2 You X H, Sheng B, Huang Y M, et al. Closed-form approximation for performance bound of finite blocklength massive MIMO transmission. 2022. ArXiv:2206.07243
3 Wang Z Q, Du Y, Wei K J, et al. Vision, application scenarios, and key technology trends for 6G mobile communications. Sci China Inf Sci, 2022, 65: 151301
4 Xu W, Yang Z H, Ng D W K, et al. Edge learning for B5G networks with distributed signal processing: semantic communication, edge computing, and wireless sensing. IEEE J Sel Top Signal Process, 2023, 17: 9–39
5 You X H, Wang C X, Huang J, et al. Towards 6G wireless communication networks: vision, enabling technologies, and new paradigm shifts. Sci China Inf Sci, 2021, 64: 110301
6 Zhang Z J, Dai L L. A joint precoding framework for wideband reconfigurable intelligent surface-aided cell-free network. IEEE Trans Signal Process, 2021, 69: 4085–4101
7 Shen D C, Dai L L, Su X, et al. Multi-beam design for near-field extremely large-scale RIS-aided wireless communications. IEEE Trans Green Commun Netw, 2023, doi: 10.1109/TGCN.2023.3259579
8 Shi W, Xu W, You X H, et al. Intelligent reflection enabling technologies for integrated and green internet-of-everything beyond 5G: communication, sensing, and security. IEEE Wireless Commun, 2023, 30: 147–154
9 Wang C X, You X H, Gao X Q, et al. On the road to 6G: visions, requirements, key technologies, and testbeds. IEEE Commun Surv Tut, 2023, 25: 905–974
10 Xing Z, Wang R, Yuan X J. Joint active and passive beamforming design for reconfigurable intelligent surface enabled integrated sensing and communication. IEEE Trans Commun, 2023, 71: 2457–2474

11 Wu Q Q, Zhang R. Intelligent reflecting surface enhanced wireless network via joint active and passive beamforming. IEEE Trans Wireless Commun, 2019, 18: 5394–5409
12 Yang L, Yang Y, Hasna M O, et al. Coverage, probability of SNR gain, and DOR analysis of RIS-aided communication systems. IEEE Wireless Commun Lett, 2020, 9: 1268–1272
13 Pan C H, Ren H, Wang K Z, et al. Multicell MIMO communications relying on intelligent reflecting surfaces. IEEE Trans Wireless Commun, 2020, 19: 5218–5233
14 Liang Y C, Chen J, Long R Z, et al. Reconfigurable intelligent surfaces for smart wireless environments: channel estimation, system design and applications in 6G networks. Sci China Inf Sci, 2021, 64: 200301
15 Sharma P K, Garg P. Intelligent reflecting surfaces to achieve the full-duplex wireless communication. IEEE Commun Lett, 2021, 25: 622–626
16 Xu D F, Yu X H, Sun Y, et al. Resource allocation for IRS-assisted full-duplex cognitive radio systems. IEEE Trans Commun, 2020, 68: 7376–7394
17 Nguyen B C, Hoang T M, Dung L T, et al. On performance of two-way full-duplex communication system with reconfigurable intelligent surface. IEEE Access, 2021, 9: 81274–81285
18 Peng Z J, Zhang Z K, Pan C H, et al. Multiuser full-duplex two-way communications via intelligent reflecting surface. IEEE Trans Signal Process, 2021, 69: 837–851
19 Xia X J, Zhu P C, Li J M, et al. Joint optimization of spectral efficiency for cell-free massive MIMO with network-assisted full duplexing. Sci China Inf Sci, 2021, 64: 182311
20 Zhang Z J, Dai L L, Chen X B, et al. Active RIS vs. passive RIS: which will prevail in 6G? IEEE Trans Commun, 2023, 71: 1707–1725
21 You C S, Zhang R. Wireless communication aided by intelligent reflecting surface: active or passive? IEEE Wireless Commun Lett, 2021, 10: 2659–2663
22 Khoshafa M H, Ngatched T M N, Ahmed M H, et al. Active reconfigurable intelligent surfaces-aided wireless communication system. IEEE Commun Lett, 2021, 25: 3699–3703
23 Zhi K D, Pan C H, Ren H, et al. Active RIS versus passive RIS: which is superior with the same power budget? IEEE Commun Lett, 2022, 26: 1150–1154
24 Long R Z, Liang Y C, Pei Y Y, et al. Active reconfigurable intelligent surface-aided wireless communications. IEEE Trans Wireless Commun, 2021, 20: 4962–4975
25 Peng Z J, Weng R S, Zhang Z K, et al. Active reconfigurable intelligent surface for mobile edge computing. IEEE Wireless Commun Lett, 2022, 11: 2482–2486
26 Dong L M, Wang H M, Bai J L. Active reconfigurable intelligent surface aided secure transmission. IEEE Trans Veh Technol, 2022, 71: 2181–2186
27 Bjornson E, Sanguinetti L. Rayleigh fading modeling and channel hardening for reconfigurable intelligent surfaces. IEEE Wireless Commun Lett, 2021, 10: 830–834
28 Zhi K D, Pan C H, Ren H, et al. Two-timescale design for reconfigurable intelligent surface-aided massive MIMO systems with imperfect CSI. IEEE Trans Inform Theor, 2023, 69: 3001–3033
29 Ngo H Q, Suraweera H A, Matthaiou M, et al. Multipair full-duplex relaying with massive arrays and linear processing. IEEE J Sel Areas Commun, 2014, 32: 1721–1737
30 Pan C H, Zhou G, Zhi K D, et al. An overview of signal processing techniques for RIS/IRS-aided wireless systems. IEEE J Sel Top Signal Process, 2022, 16: 883–917
31 Ye Z, Pan C H, Zhu H L, et al. Tradeoff caching strategy of the outage probability and fronthaul usage in a cloud-RAN. IEEE Trans Veh Technol, 2018, 67: 6383–6397
32 Zhang Q, Jin S, Wong K K, et al. Power scaling of uplink massive MIMO systems with arbitrary-rank channel means. IEEE J Sel Top Signal Process, 2014, 8: 966–981

Appendix A Proof of Theorem 1

The LMMSE estimation of the cascaded channel $q_{ii'}$ is formulated as

$$\hat{q}_{ii'} = \mathbb{E}\left\{q_{ii'}\right\} + \mathrm{Cov}\left\{q_{ii'}, y_i^{\mathrm{p}}\right\} \mathrm{Cov}^{-1}\left\{y_i^{\mathrm{p}}, y_i^{\mathrm{p}}\right\} \left(y_i^{\mathrm{p}} - \mathbb{E}\left\{y_i^{\mathrm{p}}\right\}\right). \tag{A1}$$

Recalling the definition of $q_{ii'}$ in (5), we can derive the first expectation in (A1) as

$$\mathbb{E}\left\{q_{ii'}\right\} = \mathbb{E}\left\{\boldsymbol{g}_{ri}^{\mathrm{T}} \boldsymbol{\Phi} \boldsymbol{\Lambda} \boldsymbol{g}_{ti'}\right\} = \bar{\boldsymbol{g}}_{ri}^{\mathrm{T}} \boldsymbol{\Phi} \boldsymbol{\Lambda} \bar{\boldsymbol{g}}_{ti'} \triangleq \epsilon_{ii'}. \tag{A2}$$

Similarly, we can obtain that

$$\mathbb{E}\left\{y_i^{\mathrm{p}}\right\} = \mathbb{E}\left\{q_{ii'}\right\} + \frac{1}{\sqrt{\tau p}} \mathbb{E}\left\{\boldsymbol{g}_{ri}^{\mathrm{T}} \boldsymbol{\Phi} \boldsymbol{\Lambda} \boldsymbol{N}_{\mathrm{F}} \boldsymbol{s}_{i'}\right\} + \frac{1}{\sqrt{\tau p}} \mathbb{E}\left\{\boldsymbol{n}_i^{\mathrm{H}} \boldsymbol{s}_{i'}\right\} = \mathbb{E}\left\{q_{ii'}\right\}. \tag{A3}$$

Appendix A.1 Derivation of $\mathrm{Cov}\{q_{ii'}, y_i^{\mathrm{p}}\}$

The covariance $\mathrm{Cov}\{q_{ii'}, y_i^{\mathrm{p}}\}$ can be rewritten as

$$\begin{aligned}
\mathrm{Cov}\left\{q_{ii'}, y_i^{\mathrm{p}}\right\} &= \mathbb{E}\left\{\left(q_{ii'} - \mathbb{E}\left\{q_{ii'}\right\}\right)\left(y_i^{\mathrm{p}} - \mathbb{E}\left\{y_i^{\mathrm{p}}\right\}\right)^{\mathrm{H}}\right\} \\
&= \mathbb{E}\left\{q_{ii'}\left(y_i^{\mathrm{p}}\right)^{\mathrm{H}} - \mathbb{E}\left\{q_{ii'}\right\}\left(y_i^{\mathrm{p}}\right)^{\mathrm{H}} - q_{ii'}\left(\mathbb{E}\left\{y_i^{\mathrm{p}}\right\}\right)^{\mathrm{H}} + \mathbb{E}\left\{q_{ii'}\right\}\left(\mathbb{E}\left\{y_i^{\mathrm{p}}\right\}\right)^{\mathrm{H}}\right\} \\
&\overset{\text{(a)}}{=} \mathbb{E}\left\{q_{ii'}\left(y_i^{\mathrm{p}}\right)^{\mathrm{H}}\right\} - \mathbb{E}\left\{q_{ii'}\right\}\mathbb{E}\left\{\left(y_i^{\mathrm{p}}\right)^{\mathrm{H}}\right\},
\end{aligned} \tag{A4}$$

where (a) exploits $\mathbb{E}\left\{y_i^{\mathrm{p}}\right\} = \mathbb{E}\left\{q_{ii'}\right\}$. Then, we can obtain that

$$\mathbb{E}\left\{q_{ii'}\left(y_i^{\mathrm{p}}\right)^{\mathrm{H}}\right\} = \mathbb{E}\left\{\left(q_{ii'}\right)\left(q_{ii'} + \frac{1}{\sqrt{\tau p}} \boldsymbol{g}_{ri}^{\mathrm{T}} \boldsymbol{\Phi} \boldsymbol{\Lambda} \boldsymbol{N}_{\mathrm{F}} \boldsymbol{s}_{i'} + \frac{1}{\sqrt{\tau p}} \boldsymbol{n}_i^{\mathrm{H}} \boldsymbol{s}_{i'}\right)^{\mathrm{H}}\right\} = \mathbb{E}\left\{\left|q_{ii'}\right|^2\right\}, \tag{A5}$$

$$\mathbb{E}\left\{q_{ii'}\right\}\mathbb{E}\left\{\left(y_i^{\mathrm{p}}\right)^{\mathrm{H}}\right\}=\left|\mathbb{E}\left\{q_{ii'}\right\}\right|^2. \tag{A6}$$

Substituting (A5) and (A6) into (A4), we have $\mathrm{Cov}\left\{q_{ii'},y_i^{\mathrm{p}}\right\}=\mathbb{E}\left\{\left|q_{ii'}\right|^2\right\}-\left|\mathbb{E}\left\{q_{ii'}\right\}\right|^2$.

Then, we can derive that

$$\begin{aligned}\mathbb{E}\left\{\left|q_{ii'}\right|^2\right\}=&\left|\epsilon_{ii'}\right|^2+\eta^2\mathbb{E}\left\{\bar{\boldsymbol{g}}_{ri}^{\mathrm{T}}\boldsymbol{\Phi}\boldsymbol{R}_{ti'}^{\frac{1}{2}}\tilde{\boldsymbol{g}}_{ti'}\tilde{\boldsymbol{g}}_{ti'}^{\mathrm{H}}\boldsymbol{R}_{ti'}^{\frac{1}{2}}\boldsymbol{\Phi}^{\mathrm{H}}\bar{\boldsymbol{g}}_{ri}^{*}\right\}\\&+\eta^2\mathbb{E}\left\{\tilde{\boldsymbol{g}}_{ri}^{\mathrm{T}}\boldsymbol{R}_{ri}^{\frac{1}{2}}\boldsymbol{\Phi}\bar{\boldsymbol{g}}_{ti'}\bar{\boldsymbol{g}}_{ti'}^{\mathrm{H}}\boldsymbol{\Phi}^{\mathrm{H}}\boldsymbol{R}_{ri}^{\frac{1}{2}}\tilde{\boldsymbol{g}}_{ri}^{*}\right\}+\eta^2\mathbb{E}\left\{\tilde{\boldsymbol{g}}_{ri}^{\mathrm{T}}\boldsymbol{R}_{ri}^{\frac{1}{2}}\boldsymbol{\Phi}\boldsymbol{R}_{ti'}^{\frac{1}{2}}\tilde{\boldsymbol{g}}_{ti'}\tilde{\boldsymbol{g}}_{ti'}^{\mathrm{H}}\boldsymbol{R}_{ti'}^{\frac{1}{2}}\boldsymbol{\Phi}^{\mathrm{H}}\boldsymbol{R}_{ri}^{\frac{1}{2}}\tilde{\boldsymbol{g}}_{ri}^{*}\right\}.\end{aligned} \tag{A7}$$

We can further calculate the first term in (A7) as

$$\begin{aligned}\left|\epsilon_{ii'}\right|^2&=\left|\bar{\boldsymbol{g}}_{ri}^{\mathrm{T}}\boldsymbol{\Phi}\boldsymbol{\Lambda}\bar{\boldsymbol{g}}_{ti'}\right|^2=\eta^2\left|\sum_{n=1}^{N}\mathrm{e}^{\mathrm{j}\phi_n}\left[\bar{\boldsymbol{g}}_{ri}\right]_n\left[\bar{\boldsymbol{g}}_{ti'}\right]_n\right|^2\\&=\eta^2\sum_{n=1}^{N}\left|\mathrm{e}^{\mathrm{j}\phi_n}[\bar{\boldsymbol{g}}_{ri}]_n[\bar{\boldsymbol{g}}_{ti'}]_n\right|^2+2\eta^2\sum_{n_1=1}^{N-1}\sum_{n_2=n_1+1}^{N}\mathrm{Re}\left\{\mathrm{e}^{\mathrm{j}\phi_{n_1}}\left[\bar{\boldsymbol{g}}_{ri}\right]_{n_1}\left[\bar{\boldsymbol{g}}_{ti'}\right]_{n_1}\mathrm{e}^{-\mathrm{j}\phi_{n_2}}\left[\bar{\boldsymbol{g}}_{ri}^{*}\right]_{n_2}\left[\bar{\boldsymbol{g}}_{ti'}^{*}\right]_{n_2}\right\}\\&=\eta^2\psi_{ii'}\bar{\Omega}_{ii'},\end{aligned} \tag{A8}$$

where

$$\bar{\Omega}_{ii'}=N+2\sum_{1\leqslant q<p\leqslant N}\cos\left(\phi_p-\phi_q+(2\pi/\lambda)\bar{\Gamma}_{p,q}^{i,i'}\right), \tag{A9}$$

$$\bar{\Gamma}_{p,q}^{i,i'}=\left(v_1\left(p\right)-v_1\left(q\right)\right)d_{\mathrm{H}}\left(\sin\theta_{ri}^{\mathrm{a}}\cos\theta_{ri}^{\mathrm{e}}+\sin\theta_{ti'}^{\mathrm{a}}\cos\theta_{ti'}^{\mathrm{e}}\right)+\left(v_2\left(p\right)-v_2\left(q\right)\right)d_{\mathrm{V}}\left(\sin\theta_{ri}^{\mathrm{e}}+\sin\theta_{ti'}^{\mathrm{e}}\right). \tag{A10}$$

Note that $\mathbb{E}\{\boldsymbol{R}_{xi}^{\frac{1}{2}}\tilde{\boldsymbol{g}}_{xi}\tilde{\boldsymbol{g}}_{xi}^{\mathrm{H}}\boldsymbol{R}_{xi}^{\frac{1}{2}}\}=\frac{\alpha_{xi}}{1+\mu_{xi}}\boldsymbol{R}_{xi}$. Then, we can further derive the second term in (A7) as

$$\begin{aligned}&\mathbb{E}\left\{\bar{\boldsymbol{g}}_{ri}^{\mathrm{T}}\boldsymbol{\Phi}\boldsymbol{R}_{ti'}^{\frac{1}{2}}\tilde{\boldsymbol{g}}_{ti'}\tilde{\boldsymbol{g}}_{ti'}^{\mathrm{H}}\boldsymbol{R}_{ti'}^{\frac{1}{2}}\boldsymbol{\Phi}^{\mathrm{H}}\bar{\boldsymbol{g}}_{ri}^{*}\right\}\\&=\frac{\alpha_{ti'}}{1+\mu_{ti'}}\mathbb{E}\left\{\bar{\boldsymbol{g}}_{ri}^{\mathrm{T}}\boldsymbol{\Phi}\boldsymbol{R}_{ti'}\boldsymbol{\Phi}^{\mathrm{H}}\bar{\boldsymbol{g}}_{ri}^{*}\right\}\\&=\frac{\alpha_{ti'}}{1+\mu_{ti'}}\left(\sum_{n=1}^{N}\mathbb{E}\left\{\left|\left[\bar{\boldsymbol{g}}_{ri}\right]_n\mathrm{e}^{\mathrm{j}\phi_n}\right|^2\right\}+2\sum_{n_1=1}^{N-1}\sum_{n_2=n_1+1}^{N}r_{n_1n_2}\mathbb{E}\left\{\mathrm{Re}\left\{\left[\bar{\boldsymbol{g}}_{ri}\right]_{n_1}\mathrm{e}^{\mathrm{j}\phi_{n_1}}\left[\bar{\boldsymbol{g}}_{ri}^{*}\right]_{n_2}\mathrm{e}^{-\mathrm{j}\phi_{n_2}}\right\}\right\}\right)\\&=\frac{\alpha_{ri}\alpha_{ti'}\mu_{ri}}{\left(1+\mu_{ri}\right)\left(1+\mu_{ti'}\right)}\hat{\Omega}_{ri}=\frac{\psi_{ii'}}{\mu_{ti'}}\hat{\Omega}_{ri},\end{aligned} \tag{A11}$$

where

$$\hat{\Omega}_{xi}=N+2\sum_{1\leqslant q<p\leqslant N}r_{pq}\cos\left(\phi_p-\phi_q+(2\pi/\lambda)\hat{\Gamma}_{p,q}^{xi}\right), \tag{A12}$$

$$\hat{\Gamma}_{p,q}^{xi}=\left(v_1\left(p\right)-v_1\left(q\right)\right)d_{\mathrm{H}}\sin\theta_{xi}^{\mathrm{a}}\cos\theta_{xi}^{\mathrm{e}}+\left(v_2\left(p\right)-v_2\left(q\right)\right)d_{\mathrm{V}}\sin\theta_{xi}^{\mathrm{e}}. \tag{A13}$$

Similarly, we have

$$\begin{aligned}&\mathbb{E}\left\{\tilde{\boldsymbol{g}}_{ri}^{\mathrm{T}}\boldsymbol{R}_{ri}^{\frac{1}{2}}\boldsymbol{\Phi}\bar{\boldsymbol{g}}_{ti'}\bar{\boldsymbol{g}}_{ti'}^{\mathrm{H}}\boldsymbol{\Phi}^{\mathrm{H}}\boldsymbol{R}_{ri}^{\frac{1}{2}}\tilde{\boldsymbol{g}}_{ri}^{*}\right\}\\&=\mathbb{E}\left\{\bar{\boldsymbol{g}}_{ti'}^{\mathrm{H}}\boldsymbol{\Phi}^{\mathrm{H}}\boldsymbol{R}_{ri}^{\frac{1}{2}}\tilde{\boldsymbol{g}}_{ri}^{*}\tilde{\boldsymbol{g}}_{ri}^{\mathrm{T}}\boldsymbol{R}_{ri}^{\frac{1}{2}}\boldsymbol{\Phi}\bar{\boldsymbol{g}}_{ti'}\right\}\\&=\mathbb{E}\left\{\bar{\boldsymbol{g}}_{ti'}^{\mathrm{H}}\boldsymbol{\Phi}^{\mathrm{H}}\boldsymbol{R}_{ri}^{\frac{1}{2}}\mathbb{E}\left\{\tilde{\boldsymbol{g}}_{ri}^{*}\tilde{\boldsymbol{g}}_{ri}^{\mathrm{T}}\right\}\boldsymbol{R}_{ri}^{\frac{1}{2}}\boldsymbol{\Phi}\bar{\boldsymbol{g}}_{ti'}\right\}\\&=\frac{\alpha_{ri}}{1+\mu_{ri}}\mathbb{E}\left\{\bar{\boldsymbol{g}}_{ti'}^{\mathrm{H}}\boldsymbol{\Phi}^{\mathrm{H}}\boldsymbol{R}_{ri}\boldsymbol{\Phi}\bar{\boldsymbol{g}}_{ti'}\right\}\\&=\frac{\alpha_{ri}}{1+\mu_{ri}}\left(\sum_{n=1}^{N}\mathbb{E}\left\{\left|\left[\bar{\boldsymbol{g}}_{ti'}\right]_n\mathrm{e}^{\mathrm{j}\phi_n}\right|^2\right\}+2\sum_{n_1=1}^{N-1}\sum_{n_2=n_1+1}^{N}r_{n_1n_2}\mathbb{E}\left\{\mathrm{Re}\left\{\left[\bar{\boldsymbol{g}}_{ti'}\right]_{n_1}\mathrm{e}^{\mathrm{j}\phi_{n_1}}\left[\bar{\boldsymbol{g}}_{ti'}^{\mathrm{H}}\right]_{n_2}\mathrm{e}^{-\mathrm{j}\phi_{n_2}}\right\}\right\}\right)\\&=\frac{\alpha_{ri}\alpha_{ti'}\mu_{ti'}}{\left(1+\mu_{ri}\right)\left(1+\mu_{ti'}\right)}\hat{\Omega}_{ti'}\\&=\frac{\psi_{ii'}}{\mu_{ri}}\hat{\Omega}_{ti'},\end{aligned} \tag{A14}$$

$$\begin{aligned}&\mathbb{E}\left\{\tilde{\boldsymbol{g}}_{ri}^{\mathrm{T}}\boldsymbol{R}_{ri}^{\frac{1}{2}}\boldsymbol{\Phi}\boldsymbol{R}_{ti'}^{\frac{1}{2}}\tilde{\boldsymbol{g}}_{ti'}\tilde{\boldsymbol{g}}_{ti'}^{\mathrm{H}}\boldsymbol{R}_{ti'}^{\frac{1}{2}}\boldsymbol{\Phi}^{\mathrm{H}}\boldsymbol{R}_{ri}^{\frac{1}{2}}\tilde{\boldsymbol{g}}_{ri}^{*}\right\}\\&=\mathbb{E}\left\{\tilde{\boldsymbol{g}}_{ri}^{\mathrm{T}}\boldsymbol{R}_{ri}^{\frac{1}{2}}\boldsymbol{\Phi}\boldsymbol{R}_{ti'}^{\frac{1}{2}}\mathbb{E}\left\{\tilde{\boldsymbol{g}}_{ti'}\tilde{\boldsymbol{g}}_{ti'}^{\mathrm{H}}\right\}\boldsymbol{R}_{ti'}^{\frac{1}{2}}\boldsymbol{\Phi}^{\mathrm{H}}\boldsymbol{R}_{ri}^{\frac{1}{2}}\tilde{\boldsymbol{g}}_{ri}^{*}\right\}\\&=\frac{\alpha_{ti'}}{1+\mu_{ti'}}\mathbb{E}\left\{\tilde{\boldsymbol{g}}_{ri}^{\mathrm{T}}\boldsymbol{R}_{ri}^{\frac{1}{2}}\boldsymbol{\Phi}\boldsymbol{R}_{ti'}\boldsymbol{\Phi}^{\mathrm{H}}\boldsymbol{R}_{ri}^{\frac{1}{2}}\tilde{\boldsymbol{g}}_{ri}^{*}\right\}\\&=\frac{\alpha_{ri}\alpha_{ti'}}{\left(1+\mu_{ri}\right)\left(1+\mu_{ti'}\right)}\left(\sum_{n=1}^{N}\mathbb{E}\left\{\left|\mathrm{e}^{\mathrm{j}\phi_n}\right|^2\right\}+2\sum_{n_1=1}^{N-1}\sum_{n_2=n_1+1}^{N}r_{n_1n_2}^2\mathbb{E}\left\{\mathrm{Re}\left\{\mathrm{e}^{\mathrm{j}\phi_{n_1}}\mathrm{e}^{-\mathrm{j}\phi_{n_2}}\right\}\right\}\right)\end{aligned}$$

$$= \frac{\alpha_{ri}\alpha_{ti'}}{(1+\mu_{ri})(1+\mu_{ti'})}\hat{\Omega}_0$$
$$= \frac{\psi_{ii'}}{\mu_{ti'}\mu_{ri}}\hat{\Omega}_0, \tag{A15}$$

where

$$\hat{\Omega}_0 = N + 2\sum_{1\leqslant q<p\leqslant N} r_{pq}^2\cos(\phi_p - \phi_q). \tag{A16}$$

Substituting (A8), (A11), (A14) and (A15) into (A7), we have

$$\mathbb{E}\left\{|q_{ii'}|^2\right\} = \mathbb{E}\left\{|\boldsymbol{g}_{ri}^{\mathrm{T}}\boldsymbol{\Phi}\boldsymbol{\Lambda}\boldsymbol{g}_{ti'}|^2\right\} = \eta^2\psi_{ii'}\left(\bar{\Omega}_{ii'} + \frac{1}{\mu_{ti'}}\hat{\Omega}_{ri} + \frac{1}{\mu_{ri}}\hat{\Omega}_{ti'} + \frac{1}{\mu_{ri}\mu_{ti'}}\hat{\Omega}_0\right) \triangleq \eta^2\xi_{ii'}. \tag{A17}$$

Finally, the covariance $\mathrm{Cov}\left\{q_{ii'}, y_i^{\mathrm{p}}\right\}$ is obtained as

$$\mathrm{Cov}\left\{q_{ii'}, y_i^{\mathrm{p}}\right\} = \eta^2\psi_{ii'}\left(\frac{1}{\mu_{ti'}}\hat{\Omega}_{ri} + \frac{1}{\mu_{ri}}\hat{\Omega}_{ti'} + \frac{1}{\mu_{ri}\mu_{ti'}}\hat{\Omega}_0\right). \tag{A18}$$

Appendix A.2 Derivation of $\mathrm{Cov}\{y_i^{\mathrm{p}}, y_i^{\mathrm{p}}\}$

The covariance $\mathrm{Cov}\left\{y_i^{\mathrm{p}}, y_i^{\mathrm{p}}\right\}$ can be rewritten as

$$\mathrm{Cov}\left\{y_i^{\mathrm{p}}, y_i^{\mathrm{p}}\right\} = \mathbb{E}\left\{y_i^{\mathrm{p}}\left(y_i^{\mathrm{p}}\right)^{\mathrm{H}}\right\} - \mathbb{E}\left\{y_i^{\mathrm{p}}\right\}\left(\mathbb{E}\left\{y_i^{\mathrm{p}}\right\}\right)^{\mathrm{H}}. \tag{A19}$$

Then, we can derive that

$$\begin{aligned}\mathbb{E}\left\{y_i^{\mathrm{p}}\left(y_i^{\mathrm{p}}\right)^{\mathrm{H}}\right\} =& \mathbb{E}\left\{\left(q_{ii'} + \frac{\boldsymbol{g}_{ri}^{\mathrm{T}}\boldsymbol{\Theta}\boldsymbol{\Lambda}\boldsymbol{N}_{\mathrm{F}}\boldsymbol{s}_{i'}}{\sqrt{\tau p}} + \frac{\boldsymbol{n}_i^{\mathrm{H}}\boldsymbol{s}_{i'}}{\sqrt{\tau p}}\right)\left(q_{ii'} + \frac{\boldsymbol{g}_{ri}^{\mathrm{T}}\boldsymbol{\Theta}\boldsymbol{\Lambda}\boldsymbol{N}_{\mathrm{F}}\boldsymbol{s}_{i'}}{\sqrt{\tau p}} + \frac{\boldsymbol{n}_i^{\mathrm{H}}\boldsymbol{s}_{i'}}{\sqrt{\tau p}}\right)^{\mathrm{H}}\right\} \\ \overset{(a)}{=}& \mathbb{E}\left\{q_{ii'}q_{ii'}^{\mathrm{H}}\right\} + \frac{1}{\tau^2 p}\mathbb{E}\left\{\boldsymbol{g}_{ri}^{\mathrm{T}}\boldsymbol{\Theta}\boldsymbol{\Lambda}\left(\|\boldsymbol{n}_{\mathrm{F},1}\|^2 + \cdots + \|\boldsymbol{n}_{\mathrm{F},\tau}\|^2\right)\boldsymbol{\Lambda}^{\mathrm{H}}\boldsymbol{\Theta}^{\mathrm{H}}\boldsymbol{g}_{ri}^{*}\right\} + \frac{1}{\tau^2 p}\mathbb{E}\left\{\boldsymbol{n}_i^{\mathrm{H}}\boldsymbol{n}_i\right\} \\ =& \mathbb{E}\left\{|q_{ii'}|^2\right\} + \frac{N\sigma_{\mathrm{F}}^2\eta^2\alpha_{ri}}{\tau p} + \frac{\sigma_i^2}{\tau p},\end{aligned} \tag{A20}$$

where (a) removes the zero expectations. Note that $\mathbb{E}\{|q_{ii'}|^2\} = \mathbb{E}\{|\boldsymbol{g}_{ri}^{\mathrm{T}}\boldsymbol{\Theta}\boldsymbol{\Lambda}\boldsymbol{g}_{ti'}|^2\}$ which is derived in (A17). Thus, we have

$$\mathbb{E}\left\{y_i^{\mathrm{p}}\left(y_i^{\mathrm{p}}\right)^{\mathrm{H}}\right\} = \eta^2\psi_{ii'}\left(\bar{\Omega}_{ii'} + \frac{1}{\mu_{ti'}}\hat{\Omega}_{ri} + \frac{1}{\mu_{ri}}\hat{\Omega}_{ti'} + \frac{1}{\mu_{ri}\mu_{ti'}}\hat{\Omega}_0\right) + \frac{N\sigma_{\mathrm{F}}^2\eta^2\alpha_{ri}}{\tau p} + \frac{\sigma_i^2}{\tau p}. \tag{A21}$$

Recalling $\mathbb{E}\left\{y_i^{\mathrm{p}}\right\} = \mathbb{E}\left\{q_{ii'}\right\} = \bar{\boldsymbol{g}}_{ri}^{\mathrm{T}}\boldsymbol{\Phi}\boldsymbol{\Lambda}\bar{\boldsymbol{g}}_{ti'}$ and substituting (A21) into (A19), we obtain that

$$\begin{aligned}\mathrm{Cov}\left\{y_i^{\mathrm{p}}, y_i^{\mathrm{p}}\right\} &= \eta^2\psi_{ii'}\left(\bar{\Omega}_{ii'} + \frac{1}{\mu_{ti'}}\hat{\Omega}_{ri} + \frac{1}{\mu_{ri}}\hat{\Omega}_{ti'} + \frac{1}{\mu_{ri}\mu_{ti'}}\hat{\Omega}_0\right) + \frac{N\sigma_{\mathrm{F}}^2\eta^2\alpha_{ri}}{p} + \frac{\sigma_i^2}{p} - \eta^2\psi_{ii'}\bar{\Omega}_{ii'} \\ &= \eta^2\psi_{ii'}\left(\frac{1}{\mu_{ti'}}\hat{\Omega}_{ri} + \frac{1}{\mu_{ri}}\hat{\Omega}_{ti'} + \frac{1}{\mu_{ri}\mu_{ti'}}\hat{\Omega}_0\right) + \frac{N\sigma_{\mathrm{F}}^2\eta^2\alpha_{ri}}{\tau p} + \frac{\sigma_i^2}{\tau p}.\end{aligned} \tag{A22}$$

Finally, the estimation of the cascaded channel $\hat{q}_{ii'}$ is obtained by substituting (A2), (A3), (A18) and (A22) into (A1), and it is written as

$$\begin{aligned}\hat{q}_{ii'} =& \mathbb{E}\left\{q_{ii'}\right\} + \mathrm{Cov}\left\{q_{ii'}, y_i^{\mathrm{p}}\right\}\mathrm{Cov}^{-1}\left\{y_i^{\mathrm{p}}, y_i^{\mathrm{p}}\right\}\left(y_i^{\mathrm{p}} - \mathbb{E}\left\{y_i^{\mathrm{p}}\right\}\right) \\ =& \epsilon_{ii'} + \frac{\eta^2\psi_{ii'}(\frac{1}{\mu_{ti'}}\hat{\Omega}_{ri} + \frac{1}{\mu_{ri}}\hat{\Omega}_{ti'} + \frac{1}{\mu_{ri}\mu_{ti'}}\hat{\Omega}_0)}{\eta^2\psi_{ii'}(\frac{1}{\mu_{ti'}}\hat{\Omega}_{ri} + \frac{1}{\mu_{ri}}\hat{\Omega}_{ti'} + \frac{1}{\mu_{ri}\mu_{ti'}}\hat{\Omega}_0) + \frac{N\sigma_{\mathrm{F}}^2\eta^2\alpha_{ri}}{p} + \frac{\sigma_i^2}{p}}\left(q_{ii'} + \frac{\boldsymbol{g}_{ri}^{\mathrm{T}}\boldsymbol{\Theta}\boldsymbol{\Lambda}\boldsymbol{N}_{\mathrm{F}}\boldsymbol{s}_{i'}}{\sqrt{p}} + \frac{\boldsymbol{n}_i\boldsymbol{s}_{i'}}{\sqrt{p}} - \epsilon_{ii}\right) \\ =& \epsilon_{ii'} + \iota_{ii'}\left(q_{ii'} + \frac{\boldsymbol{g}_{ri}^{\mathrm{T}}\boldsymbol{\Theta}\boldsymbol{\Lambda}\boldsymbol{N}_{\mathrm{F}}\boldsymbol{s}_{i'}}{\sqrt{p}} + \frac{\boldsymbol{n}_i\boldsymbol{s}_{i'}}{\sqrt{p}} - \epsilon_{ii}\right).\end{aligned} \tag{A23}$$

Appendix B Proof of Lemma 1

From (14), we can derive that

$$\mathbb{E}\{\|\boldsymbol{\Lambda}\boldsymbol{\Phi}\boldsymbol{g}_{ti}\|^2\} = \mathbb{E}\{\boldsymbol{g}_{ti}^{\mathrm{H}}\boldsymbol{\Phi}^{\mathrm{H}}\boldsymbol{\Lambda}^{\mathrm{H}}\boldsymbol{\Lambda}\boldsymbol{\Phi}\boldsymbol{g}_{ti}\} = \eta^2\mathbb{E}\{\boldsymbol{g}_{ti}^{\mathrm{H}}\boldsymbol{g}_{ti}\} = \eta^2\left(\mathbb{E}\{\bar{\boldsymbol{g}}_{ti}^{\mathrm{H}}\bar{\boldsymbol{g}}_{ti}\} + \mathbb{E}\{\tilde{\boldsymbol{g}}_{ti}^{\mathrm{H}}\boldsymbol{R}_{ti}\tilde{\boldsymbol{g}}_{ti}\}\right). \tag{B1}$$

Then, we calculate the first term in (B1) as

$$\mathbb{E}\{\bar{\boldsymbol{g}}_{ti}^{\mathrm{H}}\bar{\boldsymbol{g}}_{ti}\} = \sum_{n=1}^{N}\left|[\bar{\boldsymbol{g}}_{ti}]_n\right|^2 = N\frac{\alpha_{ti}\mu_{ti}}{1+\mu_{ti}}. \tag{B2}$$

Next, we have

$$\begin{aligned}\mathbb{E}\{\tilde{\boldsymbol{g}}_{ti}^{\mathrm{H}}\boldsymbol{R}_{ti}\tilde{\boldsymbol{g}}_{ti}\} &= \sum_{n=1}^{N}\mathbb{E}\left\{\left|[\tilde{\boldsymbol{g}}_{ti}]_n\right|^2\right\} + 2\sum_{n_1=1}^{N-1}\sum_{n_2=n_1+1}^{N} r_{n_1n_2}\mathbb{E}\left\{\mathrm{Re}\left\{[\tilde{\boldsymbol{g}}_{ti}]_{n_1}\left[\tilde{\boldsymbol{g}}_{ti}^{*}\right]_{n_2}\right\}\right\}\\ &\overset{\text{(a)}}{=} \sum_{n=1}^{N}\mathbb{E}\left\{\left|[\tilde{\boldsymbol{g}}_{ti}]_n\right|^2\right\} = N\frac{\alpha_{ti}}{1+\mu_{ti}},\end{aligned} \tag{B3}$$

where step (a) is based on the derivation given by

$$\mathbb{E}\left\{\mathrm{Re}\left\{[\tilde{\boldsymbol{g}}_{ti}]_{n_1}\left[\tilde{\boldsymbol{g}}_{ti}^{*}\right]_{n_2}\right\}\right\} = \mathrm{Re}\left\{\mathbb{E}\left\{[\tilde{\boldsymbol{g}}_{ti}]_{n_1}\left[\tilde{\boldsymbol{g}}_{ti}^{*}\right]_{n_2}\right\}\right\} = \mathrm{Re}\left\{\mathbb{E}\left\{[\tilde{\boldsymbol{g}}_{ti}]_{n_1}\right\}\mathbb{E}\left\{\left[\tilde{\boldsymbol{g}}_{ti}^{*}\right]_{n_2}\right\}\right\} = 0. \tag{B4}$$

Substituting (B2), (B3) into (B1), we arrive at

$$\mathbb{E}\{\|\boldsymbol{\Lambda}\boldsymbol{\Phi}\boldsymbol{g}_{ti}\|^2\} = \eta^2\left(N\frac{\alpha_{ti}\mu_{ti}}{1+\mu_{ti}} + N\frac{\alpha_{ti}}{1+\mu_{ti}}\right) = \eta^2 N\alpha_{ti}. \tag{B5}$$

The second expectation in (14) is derived below.

$$\mathbb{E}\left\{\|\boldsymbol{\Lambda}\boldsymbol{\Phi}\boldsymbol{n}_{\mathrm{F}}\|^2\right\} = \mathbb{E}\{\boldsymbol{n}_{\mathrm{F}}^{\mathrm{H}}\boldsymbol{\Phi}^{\mathrm{H}}\boldsymbol{\Lambda}^{\mathrm{H}}\boldsymbol{\Lambda}\boldsymbol{\Phi}\boldsymbol{n}_{\mathrm{F}}\} = \eta^2\mathbb{E}\{\boldsymbol{n}_{\mathrm{F}}^{\mathrm{H}}\boldsymbol{n}_{\mathrm{F}}\} = \eta^2\sum_{n=1}^{N}\mathbb{E}\left\{\left|[\boldsymbol{n}_{\mathrm{F}}]_n\right|^2\right\} = \eta^2 N\sigma_{\mathrm{F}}^2. \tag{B6}$$

Finally, substituting (B5) and (B6) into (14), we obtain (16) and complete the proof.

Appendix C Proof of Theorem 2

Applying [32, Lemma 1], the ACR of U_i in (13) can be approximated by

$$R_i \approx \log_2\left(1+\frac{P_{i'}\mathbb{E}\left\{|\hat{q}_{ii'}|^2\right\}}{P_{i'}\mathbb{E}\left\{|q_{ii'}-\hat{q}_{ii'}|^2\right\}+\sum_{k\neq i'}^{2K}\rho_1 P_k\mathbb{E}\left\{|q_{ik}|^2\right\}+\sum_{\{k,i\}\in\mathcal{S}_k}\rho_2 P_k\mathbb{E}\left\{|h_{ik}|^2\right\}+\mathbb{E}\{\left\|\boldsymbol{g}_{ri}^{\mathrm{T}}\boldsymbol{\Lambda}\boldsymbol{\Phi}\right\|^2\}\sigma_{\mathrm{F}}^2+\sigma_i^2}\right). \tag{C1}$$

Exploiting Theorem 1, we can derive that

$$\begin{aligned}\mathbb{E}\left\{|\hat{q}_{ii'}|^2\right\} =& \mathbb{E}\left\{\left|\epsilon_{ii'}+\iota_{ii'}\left(q_{ii'}+\frac{\boldsymbol{g}_{ri}^{\mathrm{T}}\boldsymbol{\Theta}\boldsymbol{\Lambda}\boldsymbol{N}_{\mathrm{F}}\boldsymbol{s}_{i'}}{\sqrt{\tau p}}+\frac{\boldsymbol{n}_i^{\mathrm{H}}\boldsymbol{s}_{i'}}{\sqrt{\tau p}}-\epsilon_{ii}\right)\right|^2\right\}\\ =& \mathbb{E}\left\{|\epsilon_{ii'}|^2\right\}+\mathbb{E}\left\{\left|\iota_{ii'}\left(q_{ii'}+\frac{\boldsymbol{g}_{ri}^{\mathrm{T}}\boldsymbol{\Theta}\boldsymbol{\Lambda}\boldsymbol{N}_{\mathrm{F}}\boldsymbol{s}_{i'}}{\sqrt{\tau p}}+\frac{\boldsymbol{n}_i^{\mathrm{H}}\boldsymbol{s}_{i'}}{\sqrt{\tau p}}-\epsilon_{ii}\right)\right|^2\right\}\\ &+2\mathrm{Re}\left\{\mathbb{E}\left\{\epsilon_{ii'}^{*}\iota_{ii'}\left(q_{ii'}+\frac{\boldsymbol{g}_{ri}^{\mathrm{T}}\boldsymbol{\Theta}\boldsymbol{\Lambda}\boldsymbol{N}_{\mathrm{F}}\boldsymbol{s}_{i'}}{\sqrt{\tau p}}+\frac{\boldsymbol{n}_i^{\mathrm{H}}\boldsymbol{s}_{i'}}{\sqrt{\tau p}}-\epsilon_{ii}\right)\right\}\right\}.\end{aligned} \tag{C2}$$

Recalling (A8), we have $\mathbb{E}\left\{|\epsilon_{ii'}|^2\right\} = \eta^2\psi_{ii'}\bar{\Omega}_{ii'}$. Then, we derive that

$$\begin{aligned}&\mathbb{E}\left\{\left|\iota_{ii'}\left(q_{ii'}+\frac{\boldsymbol{g}_{ri}^{\mathrm{T}}\boldsymbol{\Theta}\boldsymbol{\Lambda}\boldsymbol{N}_{\mathrm{F}}\boldsymbol{s}_{i'}}{\sqrt{\tau p}}+\frac{\boldsymbol{n}_i^{\mathrm{H}}\boldsymbol{s}_{i'}}{\sqrt{\tau p}}-\epsilon_{ii}\right)\right|^2\right\}\\ &= |\iota_{ii'}|^2\,\mathbb{E}\left\{\left|\left(\tilde{\boldsymbol{g}}_{ri}^{\mathrm{T}}\boldsymbol{R}_{ri}^{\frac{1}{2}}\boldsymbol{\Theta}\boldsymbol{\Lambda}\boldsymbol{R}_{ti'}^{\frac{1}{2}}\tilde{\boldsymbol{g}}_{ti'}+\tilde{\boldsymbol{g}}_{ri}^{\mathrm{T}}\boldsymbol{R}_{ri}^{\frac{1}{2}}\boldsymbol{\Theta}\boldsymbol{\Lambda}\bar{\boldsymbol{g}}_{ti'}+\bar{\boldsymbol{g}}_{ri}^{\mathrm{T}}\boldsymbol{\Theta}\boldsymbol{\Lambda}\boldsymbol{R}_{ti'}^{\frac{1}{2}}\tilde{\boldsymbol{g}}_{ti'}+\frac{\boldsymbol{g}_{ri}^{\mathrm{T}}\boldsymbol{\Theta}\boldsymbol{\Lambda}\boldsymbol{N}_{\mathrm{F}}\boldsymbol{s}_{i'}}{\sqrt{\tau p}}+\frac{\boldsymbol{n}_i^{\mathrm{H}}\boldsymbol{s}_{i'}}{\sqrt{\tau p}}\right)\right|^2\right\}\\ &= |\iota_{ii'}|^2\left(\mathbb{E}\left\{\left|\tilde{\boldsymbol{g}}_{ri}^{\mathrm{T}}\boldsymbol{R}_{ri}^{\frac{1}{2}}\boldsymbol{\Theta}\boldsymbol{\Lambda}\boldsymbol{R}_{ti'}^{\frac{1}{2}}\tilde{\boldsymbol{g}}_{ti'}\right|^2\right\}+\mathbb{E}\left\{\left|\tilde{\boldsymbol{g}}_{ri}^{\mathrm{T}}\boldsymbol{R}_{ri}^{\frac{1}{2}}\boldsymbol{\Theta}\boldsymbol{\Lambda}\bar{\boldsymbol{g}}_{ti'}\right|^2\right\}+\mathbb{E}\left\{\left|\bar{\boldsymbol{g}}_{ri}^{\mathrm{T}}\boldsymbol{\Theta}\boldsymbol{\Lambda}\boldsymbol{R}_{ti'}^{\frac{1}{2}}\tilde{\boldsymbol{g}}_{ti'}\right|^2\right\}+\frac{N\sigma_{\mathrm{F}}^2\eta^2\alpha_{ri}}{\tau p}+\frac{\sigma_i^2}{\tau p}\right)\\ &= |\iota_{ii'}|^2\left(\eta^2\psi_{ii'}\left(\frac{1}{\mu_{ti'}}\hat{\Omega}_{ri}+\frac{1}{\mu_{ri}}\hat{\Omega}_{ti'}+\frac{1}{\mu_{ri}\mu_{ti'}}\hat{\Omega}_0\right)+\frac{N\sigma_{\mathrm{F}}^2\eta^2\alpha_{ri}}{\tau p}+\frac{\sigma_i^2}{\tau p}\right),\end{aligned} \tag{C3}$$

$$\mathbb{E}\left\{\epsilon_{ii'}^{*}\iota_{ii'}\left(q_{ii'}+\frac{\boldsymbol{g}_{ri}^{\mathrm{T}}\boldsymbol{\Theta}\boldsymbol{\Lambda}\boldsymbol{N}_{\mathrm{F}}\boldsymbol{s}_{i'}}{\sqrt{\tau p}}+\frac{\boldsymbol{n}_i^{\mathrm{H}}\boldsymbol{s}_{i'}}{\sqrt{\tau p}}-\epsilon_{ii}\right)\right\} = \epsilon_{ii'}^{*}\iota_{ii'}\left(\mathbb{E}\left\{q_{ii'}\right\}-\epsilon_{ii}\right) = 0. \tag{C4}$$

Substituting (A8), (C3) and (C4) into (C2), we arrive at

$$\begin{aligned}\mathbb{E}\left\{|\hat{q}_{ii'}|^2\right\} =& \eta^2\psi_{ii'}\bar{\Omega}_{ii'}+|\iota_{ii'}|^2\left(\eta^2\psi_{ii'}\left(\frac{1}{\mu_{ti'}}\hat{\Omega}_{ri}+\frac{1}{\mu_{ri}}\hat{\Omega}_{ti'}+\frac{1}{\mu_{ri}\mu_{ti'}}\hat{\Omega}_0\right)+\frac{N\sigma_{\mathrm{F}}^2\eta^2\alpha_{ri}}{\tau p}+\frac{\sigma_i^2}{\tau p}\right)\\ =& \eta^2\varsigma_{ii'}+|\iota_{ii'}|^2\left(\frac{N\sigma_{\mathrm{F}}^2\eta^2\alpha_{ri}}{\tau p}+\frac{\sigma_i^2}{\tau p}\right).\end{aligned} \tag{C5}$$

Next, we calculate $\mathbb{E}\left\{|q_{ii'}-\hat{q}_{ii'}|^2\right\}$ which is rewritten as

$$\mathbb{E}\left\{|q_{ii'}-\hat{q}_{ii'}|^2\right\} = \mathbb{E}\left\{|q_{ii'}|^2\right\}+\mathbb{E}\left\{|\hat{q}_{ii'}|^2\right\}-2\mathrm{Re}\left\{\mathbb{E}\left\{q_{ii'}^{*}\hat{q}_{ii'}\right\}\right\}. \tag{C6}$$

We can further obtain that

$$\begin{aligned}\mathbb{E}\left\{q_{ii'}^{*}\hat{q}_{ii'}\right\}&=\mathbb{E}\left\{q_{ii'}^{*}\left(\epsilon_{ii'}+\iota_{ii'}\left(q_{ii'}+\frac{\boldsymbol{g}_{ri}^{\mathrm{T}}\boldsymbol{\Theta}\boldsymbol{\Lambda}\boldsymbol{N}_{\mathrm{F}}\boldsymbol{s}_{i'}}{\sqrt{\tau p}}+\frac{\boldsymbol{n}_{i}^{\mathrm{H}}\boldsymbol{s}_{i'}}{\sqrt{\tau p}}-\epsilon_{ii}\right)\right)\right\}\\&=\epsilon_{ii'}\mathbb{E}\left\{q_{ii'}^{*}\right\}+\iota_{ii'}\mathbb{E}\left\{\left|q_{ii'}\right|^{2}\right\}-\iota_{ii'}\epsilon_{ii'}\mathbb{E}\left\{q_{ii'}^{*}\right\}\\&\overset{(a)}{=}\left|\epsilon_{ii'}\right|^{2}+\iota_{ii'}\left(\mathbb{E}\left\{\left|q_{ii'}\right|^{2}\right\}-\left|\epsilon_{ii'}\right|^{2}\right),\end{aligned}\tag{C7}$$

where (a) uses $\mathbb{E}\left\{q_{ii'}^{*}\right\}=\left(\mathbb{E}\left\{q_{ii'}\right\}\right)^{*}=\epsilon_{ii'}^{*}$. Substituting (A17), (C5) and (C7) into (C6), we arrive at

$$\begin{aligned}\mathbb{E}\left\{\left|q_{ii'}-\hat{q}_{ii'}\right|^{2}\right\}=&\eta^{2}\xi_{ii'}+\eta^{2}\varsigma_{ii'}-2\left(\left(1-\iota_{ii'}\right)\eta^{2}\psi_{ii'}\bar{\Omega}_{ii'}+\iota_{ii'}\eta^{2}\xi_{ii'}\right)+\left|\iota_{ii'}\right|^{2}\left(\frac{N\sigma_{\mathrm{F}}^{2}\eta^{2}\alpha_{ri}}{\tau p}+\frac{\sigma_{i}^{2}}{\tau p}\right)\\=&\eta^{2}\varrho_{ii'}+\left|\iota_{ii'}\right|^{2}\left(\frac{N\sigma_{\mathrm{F}}^{2}\eta^{2}\alpha_{ri}}{\tau p}+\frac{\sigma_{i}^{2}}{\tau p}\right).\end{aligned}\tag{C8}$$

Then, we can derive $\mathbb{E}\{\|\boldsymbol{g}_{ri}^{\mathrm{T}}\boldsymbol{\Lambda}\boldsymbol{\Phi}\|^{2}\}$ similarly to (B1) as

$$\mathbb{E}\left\{\left\|\boldsymbol{g}_{ri}^{\mathrm{T}}\boldsymbol{\Lambda}\boldsymbol{\Phi}\right\|^{2}\right\}=\mathbb{E}\{\boldsymbol{g}_{ri}^{\mathrm{H}}\boldsymbol{\Lambda}^{\mathrm{H}}\boldsymbol{\Phi}^{\mathrm{H}}\boldsymbol{\Phi}\boldsymbol{\Lambda}\boldsymbol{g}_{ri}\}=\eta^{2}\mathbb{E}\{\boldsymbol{g}_{ri}^{\mathrm{H}}\boldsymbol{g}_{ri}\}=\eta^{2}N\alpha_{ri}.\tag{C9}$$

The proof is completed after substituting (A17), (C5), (C8) and (C9) into (C1).